Cell Stress and Chaperones (2018) 23:857–869
https://doi.org/10.1007/s12192-018-0893-2

ORIGINAL PAPER

Scopoletin intervention in pancreatic endoplasmic reticulum stress induced by lipotoxicity

Kalaivanan Kalpana[1] · Emayavaramban Priyadarshini[1] · S. Sreeja[1] · Kalivarathan Jagan[1] · Carani Venkatraman Anuradha[1]

Received: 10 January 2018 / Revised: 3 March 2018 / Accepted: 12 March 2018 / Published online: 25 March 2018

Abstract

Endoplasmic reticulum (ER), a dynamic organelle, plays an essential role in organizing the signaling pathways involved in cellular adaptation, resilience, and survival. Impairment in the functions of ER occurs in a variety of nutritive disorders including obesity and type 2 diabetes. Here, we hypothesize that (scopoletin) SPL, a coumarin, has the potential to alleviate ER stress induced in vitro and in vivo models by lipotoxicity. To test this hypothesis, the ability of SPL to restore the levels of proteins of ER stress was analyzed. Rat insulinoma 5f (RIN5f) cells and Sprague Dawley rats were the models used for this study. Groups of control and high-fat, high-fructose diet (HFFD)-fed rats were treated with either SPL or 4-phenylbutyric acid. Status of ER stress was enumerated by quantitative RT-PCR, Western blot, electron microscopic, and immunohistochemical studies. Proximal proteins of ER stress inositol requiring enzyme 1 (IRE1), protein kinase like endoplasmic reticulum kinase (PERK), and activating transcription factor 6 (ATF6) were reduced in the β-cells by SPL. The subsequent signaling proteins X-box binding protein 1, eukaryotic initiation factor2α, activating transcription factor 4, and C/EBP homologous protein were also suppressed in their expression levels when treated with SPL. IRE1, PERK signaling leads to c-Jun-N-terminal kinases phosphorylation, a kinase that interrupts insulin signaling, which was also reverted upon scopoletin treatment. Finally, we confirm that SPL has the ability to suppress the stress proteins and limit pancreatic ER stress which might help in delaying the progression of insulin resistance.

Keywords Scopoletin · ER stress · 4-Phenylbutyric acid · Lipotoxicity

Introduction

Endoplasmic reticulum (ER) is the primary organelle for the maturation of newly formed proteins (Gao et al. 2012). Mature proteins that exit ER proceed through the secretory pathway while the misfolded proteins are transported back to the cytosol for degradation (Meusser et al. 2005). Modifications in ER homeostasis caused by an increase in protein synthesis, hoarding of misfolded proteins, or changes in oxidative stress balance lead to ER stress (Ron and Walter 2007). Cells undergo activation of an adaptive signaling pathway called the unfolded protein response (UPR) as a response to manage ER stress. Inositol requiring enzyme-1 (IRE1), RNA-dependent protein kinase like endoplasmic reticulum kinase (PERK), and activating transcription factor-6 (ATF6) are the three major transmembrane ER sensors of misfolded proteins that initiate UPR signaling. They sense the unfolded proteins loaded in the ER lumen and pass this information across the ER membrane to the cytosol (Back and Kaufman 2012). The lumen of the ER also contains molecular chaperones and folding enzymes like glucose regulatory protein (GRP), protein disulphide isomerase-a3 (Pdia3), calnexin (Canx), and calreticulin (Calr) for protein folding (Ron and Walter 2007). Initially, cells adapt themselves to the accumulated unfolded proteins by elevating the concentration of chaperones present in the ER lumen, namely the GRP78 and GRP94 (Adamopoulos et al. 2014). The dissociation of GRP78 ameliorates the accumulation of unfolded proteins in the ER (Lee 2005; Rutkowski and Kaufman 2007; Kim et al. 2008) and upon separation of the three sensor proteins from GRP78 initiates the UPR signaling cascades. IRE1 initiates X-box binding protein-1 (XBP1), a transcription factor regulating UPR-associated genes (Lee et al. 2003; Yoshida

✉ Carani Venkatraman Anuradha
cvaradha@yahoo.com

[1] Department of Biochemistry and Biotechnology, Annamalai University, Annamalai Nagar, Tamil Nadu 608002, India

et al. 2001); PERK decreases translational initiation by inactivating eukaryotic initiation factor-2α (eIF2α) and activates ATF4 (Kadowaki and Nishitoh 2013); ATF6 gets cleaved in Golgi and transferred to the nucleus in its activated form (Ye et al. 2000). These changes are linked with the activation of c-Jun-N-terminal kinases (JNK) that phosphorylates insulin receptor substrate-1 (IRS1), which interferes in insulin signaling. Previous studies evidenced that ER stress proteins—GRP78, XBP1s, eIF2α—and inflammatory kinase protein JNK are elevated in the liver and adipose tissues of obese insulin resistant non-diabetic humans (Boden et al. 2008) but attained normalcy after gastric bypass-induced weight loss (Gregor et al. 2009).

Given the importance of ER stress signaling in metabolic pathways, our current aim is to examine UPR-mediated pancreatic stress in high-fat, high-fructose diet (HFFD)-fed Sprague Dawley rats, a physiologically relevant model for obesity and type 2 diabetes (T2D). We have extensively used this diet model to test the preventive and therapeutic potential of a wide range of phytochemicals and medicinal plants in our laboratory (Yogalakshmi et al. 2014; Kalivarathan et al. 2017). We challenged rats with HFFD to create a nutrient excess environment that in turn develops stress in ER. Scopoletin (SPL) (6-methoxy-7-hydroxycoumarin) possesses various pharmacological properties, such as anti-inflammatory, hypo-uricemic, and antioxidant activities (Moon et al. 2007; Siatka and Kasparova 2008; Mogana et al. 2013; Panda and Kar 2006). SPL has been show to improve the sensitivity of liver cells to insulin and the cellular metabolism of glucose and lipids in high fat diet-fed C57BL/6J mice, a model of fatty liver (Ham et al. 2016). Therefore, we assessed the in vivo effect of SPL on ER stress during nutrient excess. Further, cell culture studies with rat insulinoma 5f (RIN5f) cell line were designed to substantiate the role of SPL in suppressing the stress developed in ER. The results demonstrate that the therapeutic potential of SPL could be possibly mediated by its modulatory effects on ER stress. Those findings derived for SPL were matched with those for 4-phenylbutyric acid (4-PBA), a well-known ER stress inhibitor.

Materials and methods

Reagents and antibodies Fructose and casein protein were procured from SFA Food and Pharma Ingredients Pvt. Ltd., Thane, Maharashtra, and Clarion Casein Pvt. Ltd., Kadi, Gujarat, respectively. Antibodies against β-actin (Catalog # sc-47778), GRP 78 (H-129): (Catalog # sc-13968), ATF6α (F-7): (Catalog # sc-166659), phospho-JNK (G-7) (Catalog # sc-6254), and JNK (D-2) (Catalog # sc-7345) were procured from Santa Cruz Biotechnology, CA, USA. Anti-IRE1 (phospho S724) antibody ab48187 was procured from Abcam, Cambridge, USA. Antibodies PERK (D11A8) Rabbit mAb (Catalog # 5683), phospho-PERK (Thr980) (16F8) Rabbit mAb (Catalog # 3179), IRE1α (14C10) Rabbit mAb (Catalog # 3294), eIF2α (D7D3) XP® Rabbit mAb (Catalog # 5324), phospho-eIF2α (Ser51) (D9G8) XP™ Rabbit mAb (Catalog # 3398), ATF4 (D4B8) Rabbit mAb (Catalog # 11815), CHOP (L63F7) Mouse mAb (Catalog # 2895), XBP1s (D2C1F) Rabbit mAb (Catalog # 12782), and HRP-conjugated secondary antibodies (anti-mouse, anti-rat, anti-rabbit, and anti-goat) were from Cell Signaling Technology, Danvers, MA, USA.

Oligonucleotide primers and power SYBR® Green PCR master mix were procured from Genei, Bengaluru, India, and Kapa Biosystems, Wilmington, MA, USA, respectively. Immobilon polyvinylidene fluoride (PVDF) membrane (Millipore, Darmstadt, Germany)-enhanced chemiluminescence (ECL) kit (Thermo Scientific Super Signal West Pico Chemiluminescent Substrate, Rockford, PA, USA) were used for immunoblotting. SPL and 4-PBA were obtained from Sigma-Aldrich Pvt. Ltd., (St Louis, MO, USA). All other reagents and solvents used were of analytical grade.

In vitro experimental paradigms

Cell culture Rat insulinoma 5f (RIN5f) cell line was obtained from National Centre for Cell Science (NCCS, Pune, India). RIN5f cells (passages 128-138) were grown in HiGlutaXL™ Roswell Park Memorial Institute (RPMI)-1640 medium supplemented with L-alanyl-L-glutamine, 4-(2-hydroxyethyl)-1-piperazineethanesulfonic acid (HEPES) buffer, 60 mg/L penicillin, 100 mg/L streptomycin, 15% fetal bovine serum (FBS), and sodium bicarbonate (HiMedia Laboratories Pvt. Ltd., Mumbai, India) in a humidified incubator at 37 °C with 5% CO_2. Cells were dislodged using trypsin (0.125%)–ethylenediaminetetraacetic acid (EDTA) (0.02%) solution.

Palmitate preparation Palmitate/bovine serum albumin (BSA) conjugate was prepared by soaping palmitate with sodium hydroxide and mixing with BSA. Palmitate (20 mM in 0.01 M NaOH) was incubated at 70 °C for 30 min. Fatty acid soaps were then complexed with 5% fatty acid free BSA in phosphate-buffered saline (PBS) at a 1:3 volume ratio. The complexed fatty acids consisted of 5 mM palmitate and 3.75% BSA. The palmitate/BSA conjugate was diluted in RPMI 1640 medium and administered to cultured cells (Jung et al. 2015).

Cell viability assay Cell viability was carried out using RIN5f cells by MTT assays (3-(4,5-dimethylthiazole-2-yl)-2,5-diphenyltetrazolium bromide) (Sigma, USA) in order to fix the dose and exposure time for palmitate, SPL, and 4-PBA. 20×10^3 cells were grown in 96-well plates for 24 h to obtain 80% confluency and then treated using fresh RPMI 1640 medium

Table 1 Primers designed for qRT-PCR reactions

S. No.	Genes	T_m	<Forward primer sequence>	<Reverse primer sequence>
1	*Ire1*	58.9 °C	5′CACAGCCCCTCTGTGGTAAC3′	5′GCTTTCACCAGGCACACTTA3′
2	*Atf6*	60.1 °C	5′ATCTCAGGTCGGGGAGTTCT3′	5′GGCGCAGGCTGTATACTGAT3′
3	*Perk*	60.0 °C	5′AGGAACATCGTAGGGGCTTT3′	5′GAGTTGCAGACCCGAGCTAC3′
4	*Calr*	60.0 °C	5′CTCAGGTCAAGTCTGGCACA3′	5′TGGCCTCTACAGCTCATCCT3′
5	*Canx*	59.9 °C	5′GGATCCCTTTGTGTGGCTAA3′	5′GAGCCTCCATGGTTCAACAG3′
6	*Pdia3*	60.2 °C	5′GGGGCTGAGGTGGAATTTAT3′	5′CTTTGGGGACACAGGACAAT3′
7	*Chop*	52.3 °C	5′GTATCTGAGAAGGGAGGAAT3′	5′CTTAAACTCCATTCCCATCC3′
Internal control				
8	*Gapdh*	60.0 °C	5′AAGGGGAACCCTTGATATGG3′	5′CGGAGATGATGACCCTTTTG3′

with serial concentrations of palmitate/BSA conjugate for 16 h. Different serial concentrations of SPL and 4-PBA were used to treat the cells induced with palmitate grown in 96-well plates. To terminate the experiments, control and test samples were incubated with 0.5 mg/ml of MTT in PBS for 4 h. The formazan crystals formed were dissolved using 10% dimethyl sulfoxide (DMSO) and absorbance was measured at 570–640 nm using an ELISA plate analyzer (Readwell Touch, Robonik, India). The

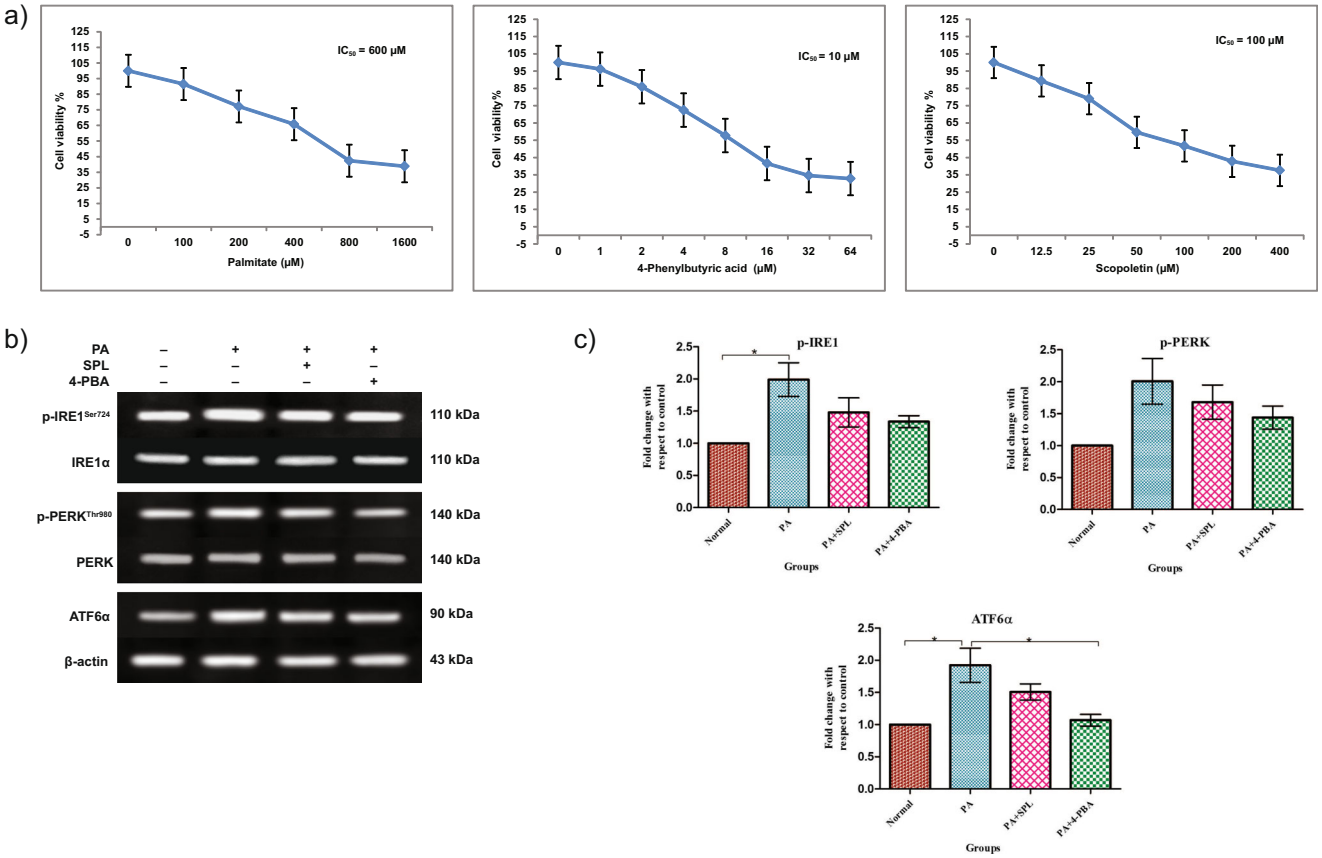

Fig. 1 Expression of ER stress canonical proteins and cytotoxicity assay in palmitate-induced RIN5f cells. Cells were treated with different serial concentrations of PA, SPL, and 4-PBA to evaluate the IC_{50} values. **a** Cytotoxicity by PA treatment (16 h) and the PA-treated RIN5f cells upon treatment with SPL and 4-PBA (24 h) was evaluated by MTT assay (mean ± SEM; $n = 3$). **b** Representative blots showing the protein bands detected by chemiluminescence signal. The top panel shows bands for pIRE1 (MW 110 kDa) normalized with total IRE1α (MW 110 kDa). The middle panel shows the bands for pPERK (MW 140 kDa) normalized with total PERK (MW 140 kDa). The bottom panel shows the bands for ATF6α (MW 90 kDa) normalized with β-actin (MW 43 kDa). Activation of the ER stress sensors was confirmed with anti-phospho-IRE1/IRE1α, phospho-PERK/PERK, and ATF6α/β-actin antibodies. **c** Densitometric analysis of Western blots as shown in **b**, normalized with their total forms and β-actin ($n = 3$). Statistical analysis was done by one-way ANOVA with Tukey's post hoc test. (Mean ± SD; $*p < 0.05$, $**p < 0.01$, $***p < 0.001$) (PA = palmitate, SPL = scopoletin, 4-PBA = 4-phenylbutyric acid)

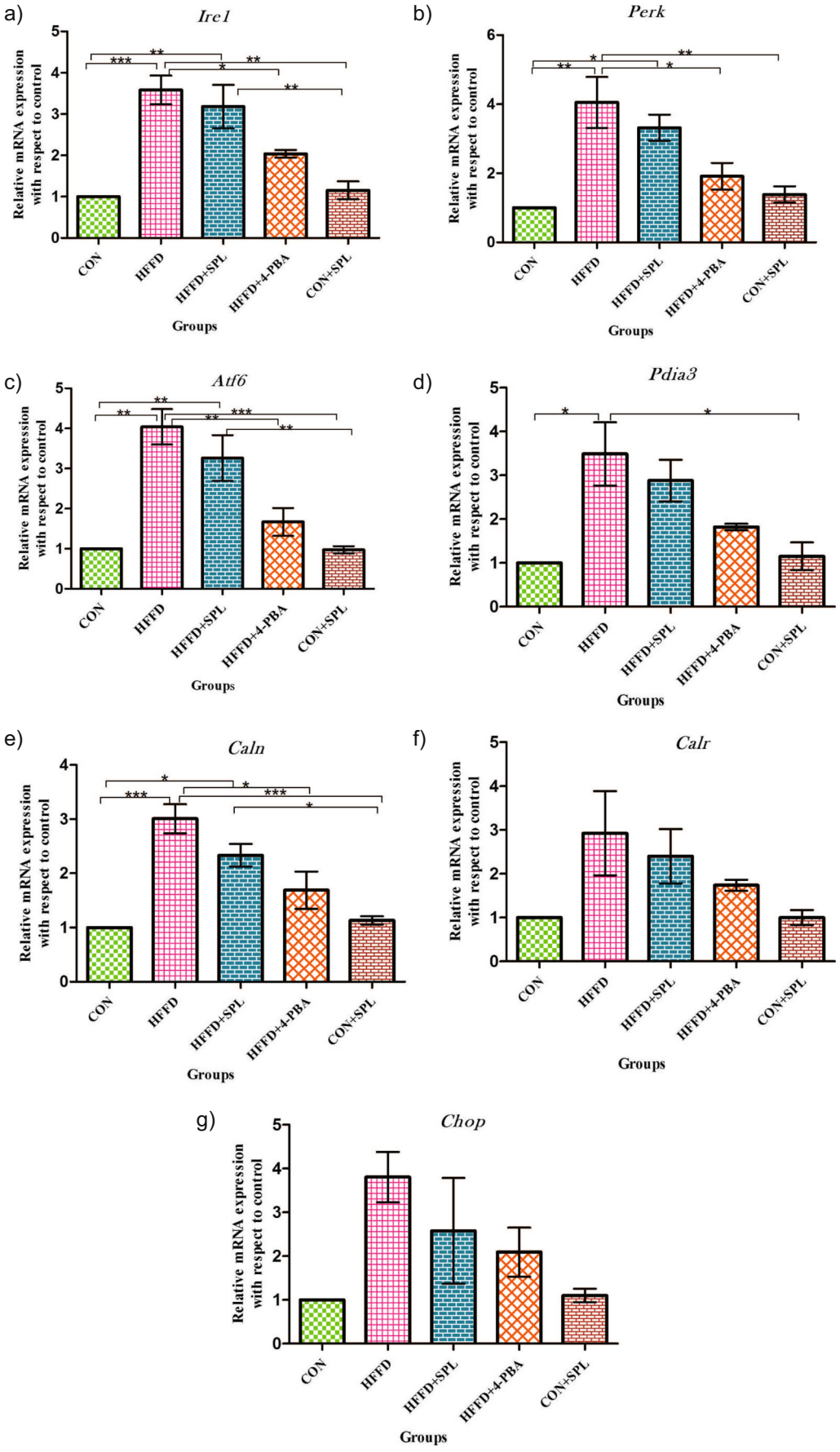
a)
Ire1
Relative mRNA expression with respect to control
Groups
CON
HFFD
HFFD+SPL
HFFD+4-PBA
CON+SPL
b)
Perk
c)
Atf6
d)
Pdia3
e)
Caln
f)
Calr
g)
Chop

◀ **Fig. 2** Quantitative real-time PCR analysis of mRNA transcripts of rat pancreas. Total pancreas mRNA from CON, HFFD, HFFD + SPL, HFFD + 4-PBA, and CON + SPL-treated Sprague Dawley rats were isolated for the PCR analysis. Expression values were normalized to GAPDH mRNA levels (**a**–**g**). Fold change of the gene expression was calculated by $2^{-\Delta\Delta Ct}$. (Mean ± SD; $n = 3$, $^{*}p < 0.05$, $^{**}p < 0.01$, $^{***}p < 0.001$) (*Ire1* = inositol requiring enzyme 1, *Perk* = PKR-like ER kinase, *Atf6* = activating transcription factor, *Pdia3* = protein disulphide isomerase a3, *Caln* = calnexin, *Calr* = calreticulin, *Chop* = C/EBP homologous protein). Abbreviations mentioned in the figures throughout denotes: CON = group of rats fed with standard pellet, HFFD = rats fed with HFFD diet alone, HFFD + SPL = HFFD-fed rats treated with SPL, HFFD + 4-PBA = HFFD-fed rats treated with 4-PBA, CON + SPL = control rats fed with standard pellet and treated with SPL

percentage of viable cell count was calculated assuming control viable cell count as 100% (Mosmann 1983).

$$\frac{\text{Mean OD of untreated cells} - \text{Mean OD of treated cells}}{\text{Mean OD of untreated cells}} \times 100$$

In vivo experimental paradigms

Experimental animals and diet composition Experiments were carried out in male Sprague Dawley rats of age 8–10 weeks old weighing between 100 and 120 g, procured from Biogen, Laboratory Animal Facility, Bengaluru, India. The experimental diet was prepared freshly every day in the laboratory with the following ingredients (g/100 g): fructose 45.0, groundnut oil 10.0, beef tallow 10.0, casein 22.5, DL-methionine 0.3, wheat bran 5.5, vitamin mixture 1.2, and mineral mixture 5.5. Standard rat pellets (Sai Enterprise, Chennai, India) composed of 60% (*w*/*w*) starch, 22.08% (*w*/*w*) protein, and 4.38% (*w*/*w*) fat provided energy of 382.61 cal/100 g, whereas HFFD provided 471.25 cal/100 g.

Animal maintenance Animals procured from Rajah Muthiah Medical College and Hospital (RMMC & H) were maintained under standard temperature (25 °C) and humidity with an alternating 12 h light/dark cycle. All the experimental procedures were approved by the Institutional Animal Ethics Committee (IAEC), Annamalai University, and conducted according to the guidelines by the Committee for the Purpose of Control and Supervision on Experiments on Animals (CPCSEA) (Proposal No. 1091). After acclimatization for a period of 1 week, the animals were randomly divided into five groups consisting of six rats ($n = 6$) each and were maintained for a period of 90 days.

Treatment procedure The rats were randomized into experimental and control groups and divided into five groups of six animals each. Animals in group 1 were the untreated rats fed with standard pellet (CON). Another set of six rats fed with HFFD served as group 2. Animals in groups 3 and 4 were fed with HFFD and treated with SPL (1 mg/kg bw/day, p.o.) (Verma et al. 2013) from day 46 till the end of experimental period and 4-PBA (1 μg/kg bw/day, i.p.) Castro et al. 2013) from day 76 till the end of experimental period, respectively. Animals in group 5 received standard pellet fed with SPL (1 mg/kg bw/day, p.o.) from day 46 till the end of experimental period.

Animal sacrifice Duration of the study period was terminated after 90 days and the rats were sacrificed by cervical dislocation after an overnight fast. Blood and pancreas tissue samples were collected and processed for analyses. A portion of the pancreas tissue was immediately frozen in liquid nitrogen for subsequent RNA extraction, while another portion was processed using lysis buffer for Western blot analysis.

RNA preparation and qRT-PCR analysis RNA was extracted from rat pancreas using TRIzol reagent (Genei, Bengaluru, India). The concentration of detected RNA was determined spectrophotometrically at 260 nm (Biophotometer plus, Eppendorf, Hamburg, Germany) and the purity of RNA preparation was checked by calculating the absorbance ratio at 260/280 nm. Quantitative real-time polymerase chain reaction (qRT-PCR) was conducted in a two-step PCR procedure. The extracted RNA (2.0 μg) was reverse transcribed by standardized procedure and the obtained cDNA was quantified (Biophotometer Plus, Eppendorf, Hamburg, Germany). After quantification, qRT-PCR amplification was performed in a 20-μL reaction mixture containing cDNA (100 ng), 1 μL each of 0.3 μM of reverse and forward primers, 10 μL Maxima SYBR Green qPCR Master Mix, and sterile water. The nucleotide sequences of primers used are given in Table 1. The PCR program was conducted using real-time PCR system Mastercycler ep realplex (Eppendorf, Hamburg, Germany) in universal cycling conditions (10 min at 95 °C, 40 cycles of 2 min at 95 °C, 30 s at 60 °C (or the optimal T_m), and 20 s at 72 °C). The target gene were normalized with an endogenous control glyceraldehyde-3-phosphate dehydrogenase (GAPDH) by using $2^{-\Delta\Delta CT}$ (Livak and Schmittgen 2001) and the relative quantity was expressed in bar graphs as fold change with respect to control.

Protein extraction and Western blotting For protein isolation, the pancreas tissue was homogenized in ice-cold homogenization buffer (20 mM Tris–HCl, pH 7.4, 0.25% SDS, 150 mM NaCl, 1% Nonidet P-40, 0.5% Triton X-100, 1 mM phenyl methyl sulfonyl fluoride (PMSF), 1 mM EDTA, and protease inhibitor cocktail) and centrifuged at 12,000×*g*, for 15 min at 4 °C. The supernatant was used as the whole cell extract. The concentrations of the extracted proteins were measured using spectrophotometer by Lowry et al. (1951). Pancreas homogenates containing equal amount of protein were resolved by 8–12% sodium dodecyl sulfate-polyacrylamide gel electrophoresis (SDS PAGE). The separated proteins were electro-transferred onto

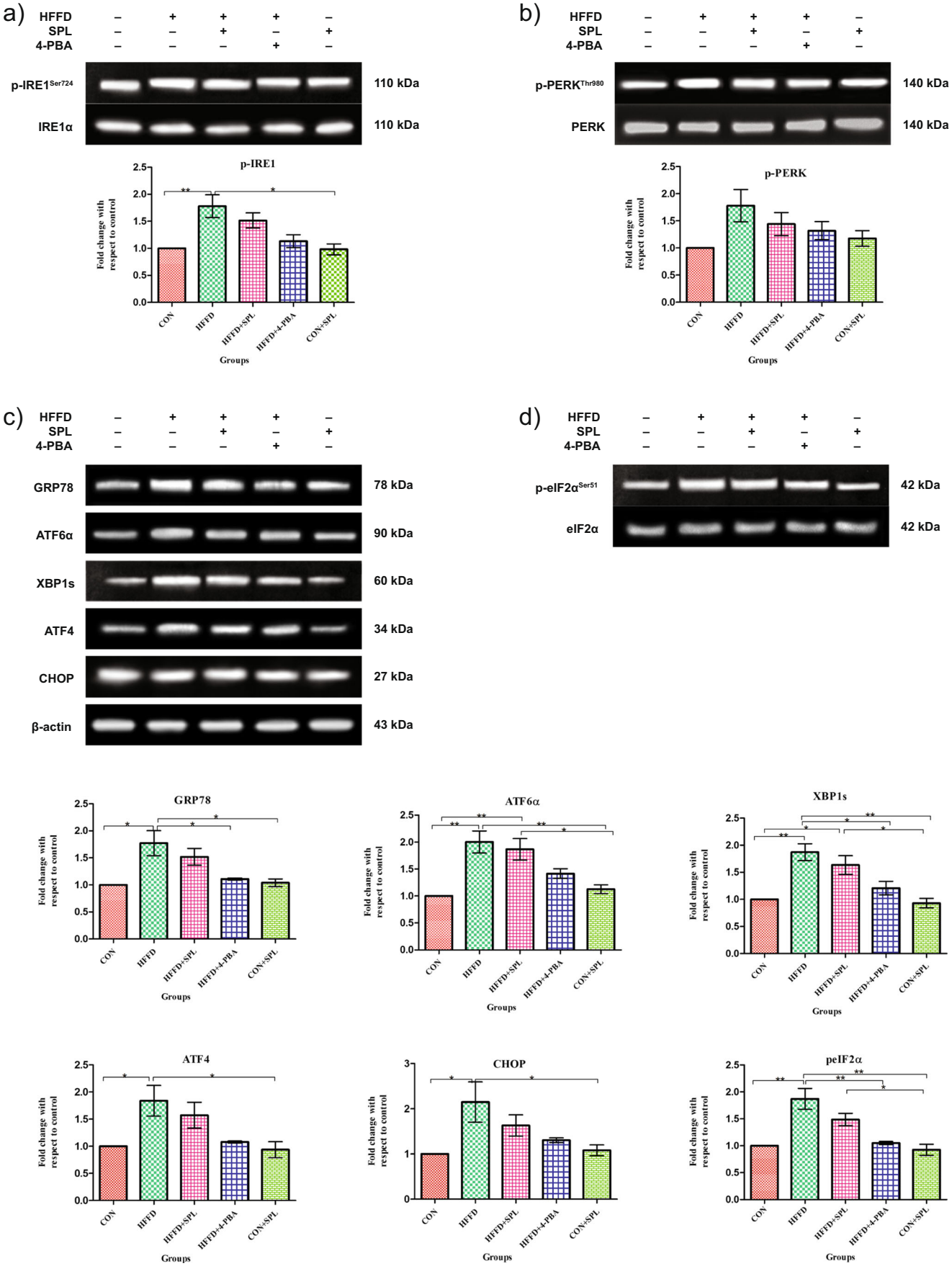
a)
HFFD
SPL
4-PBA
p-IRE1Ser724
IRE1α
110 kDa
110 kDa
p-IRE1
Fold change with respect to control
CON
HFFD
HFFD+SPL
HFFD+4-PBA
CON+SPL
Groups
b)
p-PERKThr980
PERK
140 kDa
140 kDa
p-PERK
c)
GRP78
ATF6α
XBP1s
ATF4
CHOP
β-actin
78 kDa
90 kDa
60 kDa
34 kDa
27 kDa
43 kDa
GRP78
ATF6α
XBP1s
ATF4
CHOP
d)
p-eIF2αSer51
eIF2α
42 kDa
42 kDa
peIF2α

◀ **Fig. 3** Immunoblotting of proteins belonging to ER stress signaling in Sprague Dawley rats. **a** Representative immunoblot analysis of ER stress proteins. In pancreas tissues of 90 days HFFD-fed rats, immunoblotting was performed using antibodies against phospho-IRE1 and IRE1α (**a**); phospho-PERK and PERK (**b**); GRP78, ATF6α, XBP1s, CHOP, and β-actin (**c**); and phospho-eIF2α and eIF2α (**d**) along with their quantification analysis performed based upon the indicated loading control (β-actin for GRP78, ATF6α, XBP1s, ATF4, CHOP, and IRE1α for phospho-IRE1, PERK for phospho-PERK, eIF2α for phospho-eIF2α). Statistical analysis in **b** was done by one-way ANOVA with Tukey's post hoc test. (Mean ± SD; $n = 3$, $^{*}p < 0.05$, $^{**}p < 0.01$, $^{***}p < 0.001$)

PVDF membrane followed by blocking in the Tris-buffered saline Tween 20 (TBST) solution (pH 7.4) containing 3% BSA for 2 h at room temperature and then incubated overnight at 4 °C with primary antibodies. After incubation, blots were washed with TBST and incubated with the respective secondary antibodies for 2 h at room temperature. Proteins were detected by chemiluminescence with an ECL kit and the images were captured using GELSTAN 1312 Chemi, a chemiluminescence and fluorescence imaging system (Medicare, Chennai, Tamil Nadu, India) followed by quantification using the Image J software (National Institute of Health Bethesda, MD, USA).

Immunohistochemical analysis For immunohistochemical analysis, the paraffin sections (4 μm) were initially baked for 1 h at 60 °C followed by dewaxing with xylene. Sections were then rehydrated with graded concentrations of isopropyl alcohol and subjected to antigen retrieval for 3 min using citrate buffer. Incubation of antigen retrieved sections in peroxide blocking reagent for 10 min and rinsing with phosphate buffer were performed. It was then followed by incubation with power block solution for 10 min. Non-specific binding was minimized by washing the sections with 3% BSA in phosphate-buffered saline for 30 min. Sections were incubated overnight with the primary antibodies. The sections rinsed with phosphate buffer and incubated with super enhancer reagent for 30 min were again rinsed with phosphate buffer. Incubation with super sensitive polymer-HRP immunohistochemistry detection system (Biogenex laboratories) was done and was trailed by washing thoroughly with phosphate buffer. The washed sections were incubated with 3,3′-diaminobenizidine (DAB) substrate solution for 5 min and counterstained with hematoxylin. The sections were photographed under the Olympus CX 41 microscope attached with digital camera Olympus micro.

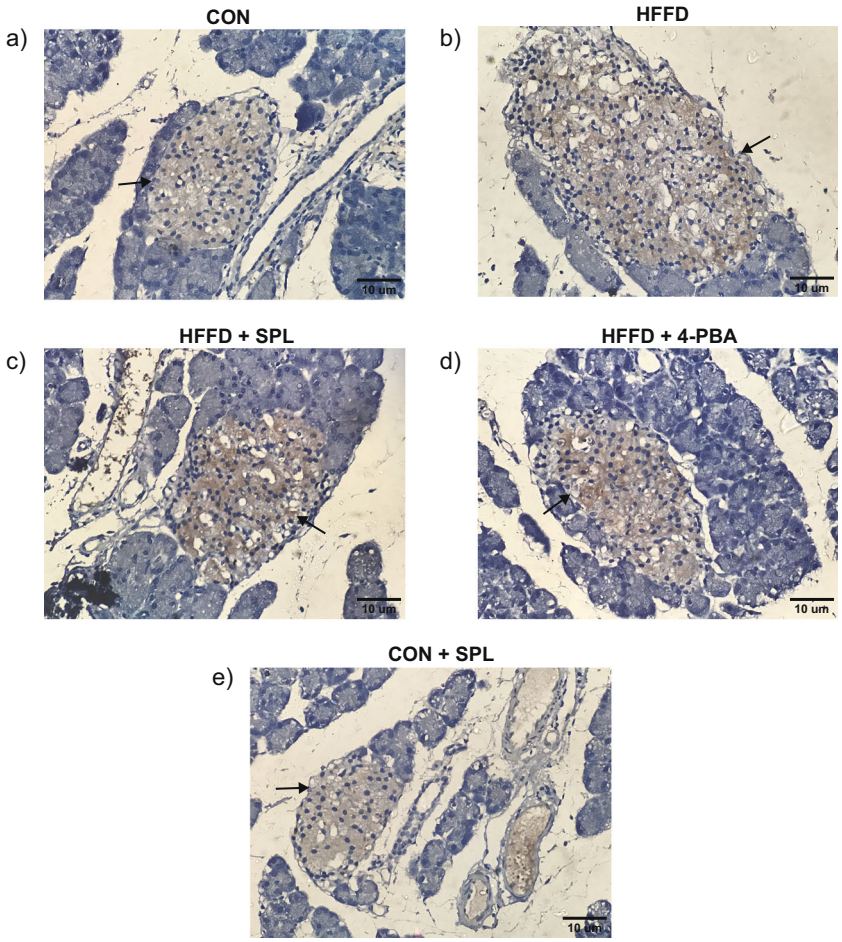

Fig. 4 Immunohistochemical localization in HFFD-fed rats. Representative photomicrographs (**a**-**e**) of immunohistochemical staining of phospho-IRE1 in control and experimental rats. Brown color indicates DAB staining and the occurrence of antigen–antibody reaction. Blue color indicates hematoxylin staining and the absence of antigen–antibody reaction. Black arrows represent immunoreactivity. Scale bars = 10 μm

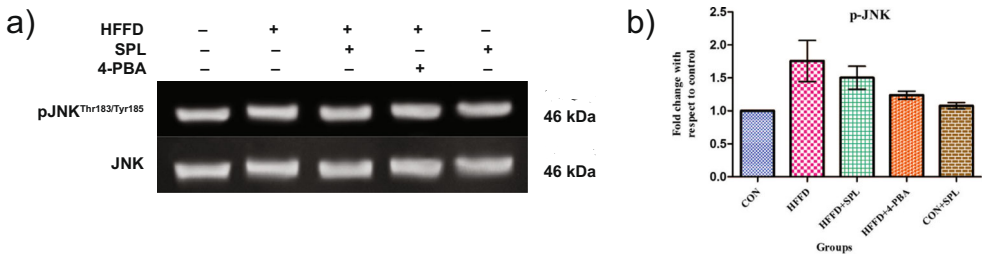

Fig. 5 Phosphorylation status of JNK. **a** Representative immunoblots of phospho- and total form of JNK. **b** Densitometric analysis was done by one-way ANOVA with Tukey's post hoc test. (Mean ± SD; $n = 3$, $^{*}p < 0.05$, $^{**}p < 0.01$, $^{***}p < 0.001$)

Transmission electron microscopic studies Pancreatic tissue removed from the animals were cut into small bits of size 1 mm^2 and fixed in 2% ice-cold glutaraldehyde for 4–8 h at 8 °C. Then it was post fixed in 0.1% osmium tetroxide for 2 h at 8 °C, dehydrated through a graded series of acetone concentrations, and embedded in Epon 812 resin with catalyst in easy molds for 48 h at 60 °C. The tissue was then sectioned using Leica Ultramicrotome with diamond or glass knives. Ultrathin sections (~ 50 nm) were mounted on copper grids, stained with 2% uranyl acetate and 0.2% lead citrate. The sections were screened in a JEOL JEM 1400 transmission electron microscope at an accelerating voltage of 80 kV equipped with an Olympus Keen view CCD camera.

Statistical analysis The values are given as means ± SD with $n = 3$ for immunoblot, qRT-PCR analysis, and histological studies. Statistical significance was examined by one-way analysis of variance (ANOVA) followed by Tukey's post hoc test using the Prism version 5.0 software (Graph Pad Software, La Jolla, CA, USA). A probability value less than 0.05 ($p < 0.05$) was considered to be significant.

Results

SPL protects RIN5f cells against palmitate-induced ER stress To elucidate the mechanism of action of SPL, we first planned for a set of in vitro experiments in RIN5f cells. Cell viability upon treatment with palmitate, SPL, and 4-PBA was assessed by MTT assay. After 16 h exposure of RIN5f cells to palmitate, 50% of cell viability was noted at a concentration of 600 μM. Palmitate-induced RIN5f cells were then treated with different serial concentrations of SPL or 4-PBA for 24 h to measure their IC_{50} values. One hundred micromolar SPL and 10 μM 4-PBA were observed to be sufficient to maintain 50% of cells as viable (Fig. 1a).

To confirm the development of ER stress in RIN5f cells, the expression of ER stress sensors IRE1α, PERK and ATF6α were measured quantitatively by Western blot. We identified that palmitate treatment decreased the expression while treatment with SPL or 4-PBA upregulated the expression of phospho-IRE1 and phospho-PERK and ATF6α levels suggesting that the treatment effectively suppressed ER stress in RIN5f cells developed by palmitate (Fig. 1b, c).

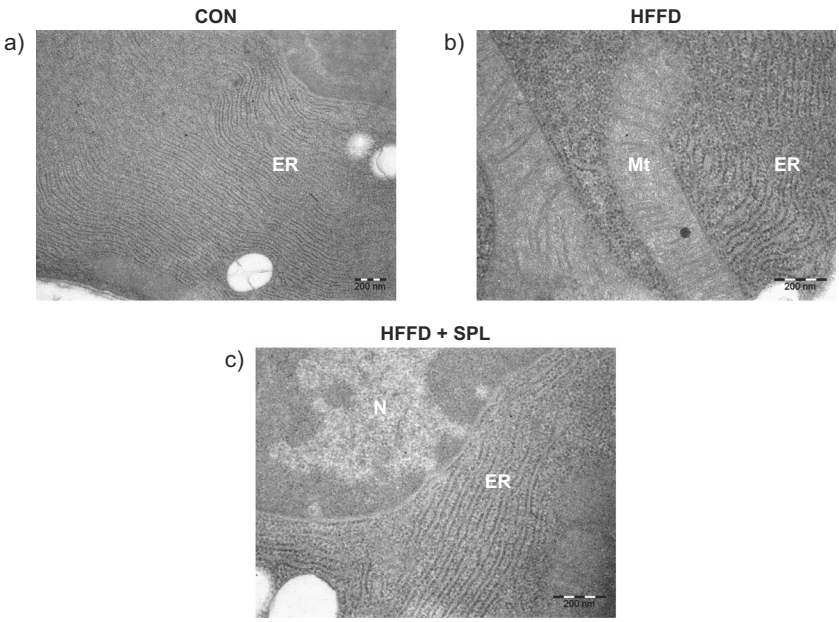

Fig. 6 Ultrastructural view of endoplasmic reticulum under transmission electron microscopic magnification. **a** Control rat pancreas shows normal ER pattern in its structure. **b** HFFD-fed rat pancreas shows high dilation in ER. **c** SPL-treated HFFD-fed rat exhibits ER architecture along with nucleus similar to control rats with little dilation. Scale bars = 200 nm

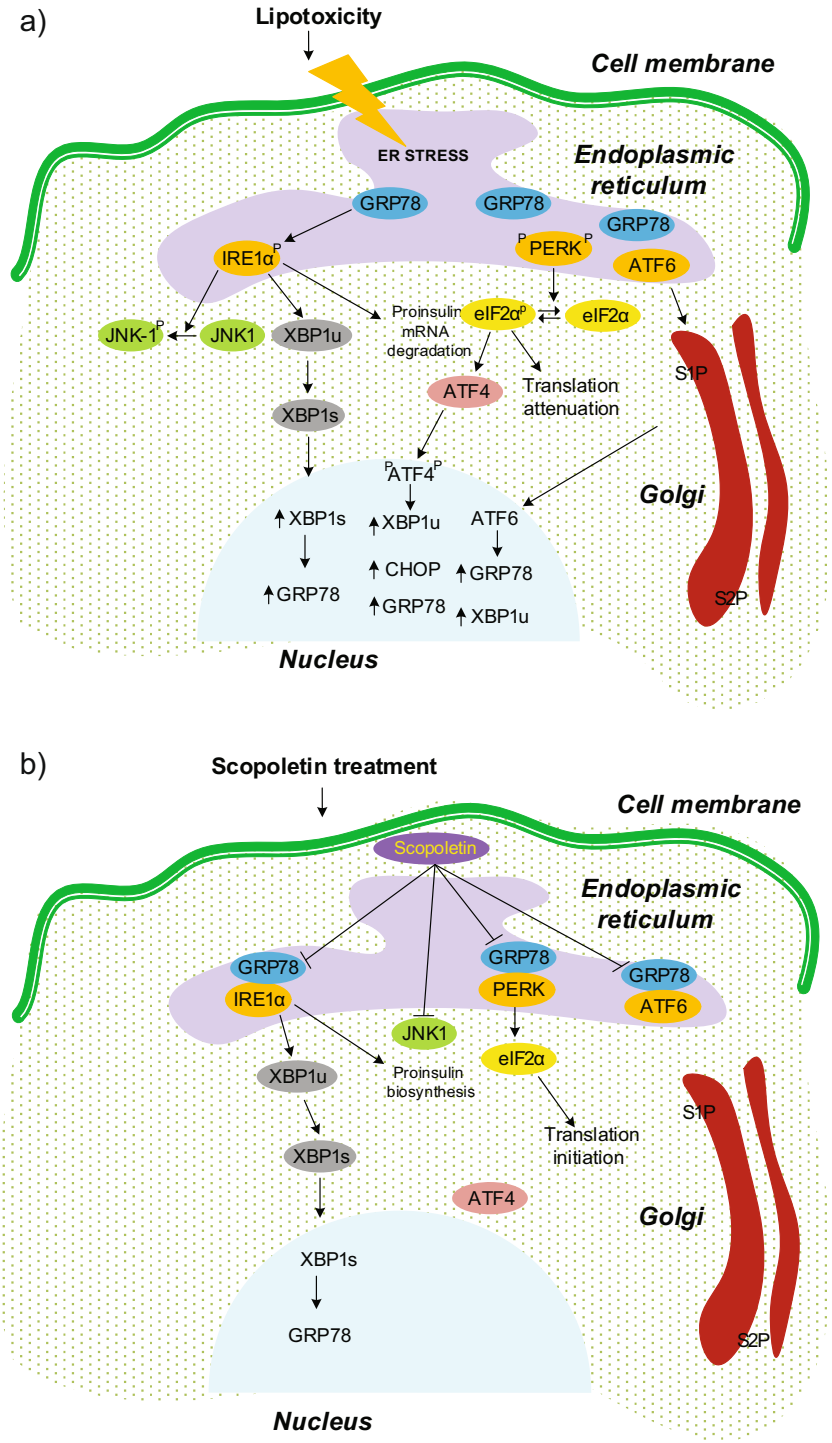

Fig. 7 Physiopathological condition of ER in rat pancreas during lipotoxicity and SPL treatment. UPR signaling that takes place in ER involves the sensor proteins IRE1α, PERK, and ATF6α associated with GRP78, a molecular chaperone that protects the cell from the accumulation of misfolded proteins. UPR signaling mechanism in basal condition: (1) IRE1α signaling—IRE1α phosphorylation cleaves XBP1 unspliced to spliced mRNA and the mRNA transcript then induces the UPR target gene GRP78. (2) PERK signaling—autophosphorylation of PERK generates phospho-eIF2α which blocks its translation initiation and induces the phosphorylation of ATF4 leading to the stimulation of gene expressions of GRP78, CHOP, and XBPu. (3) ATF6 signaling—includes its translocation to Golgi for proteolytic cleavage by site-1 protease (S1P) and site-2 protease (S2P). Its subsequent release into the nucleus enables to induce expression of GRP78 and XBP1u. **a** Lipotoxicity: In lipotoxic cells, accumulated misfolded proteins have higher affinity for GRP78 and gets dissociated enabling the initiation of the UPR signaling cascades. Increased ER chaperones blocks the phosphorylation of eIF2α and the splicing of XBP1, and the signaling proteins involved in the UPR signaling balances the cells towards stress. Spliced XBP1 then initiates the phosphorylation of JNK at threonine 183/tyrosine 185. **b** Scopoletin treatment: Upon treatment with scopoletin, the transducers are found to rebound with GRP78 and maintain the ER homeostasis, thereby deactivating JNK

SPL alleviates mRNA of ER stress molecular chaperones To further explore the mechanism for the protective effect of SPL, we then moved on to in vivo experiments. Stress was developed in rodents by feeding with high-fat along with high-fructose diet. Gene expression of *Ire1*, *Perk*, *Atf6*, and molecular chaperones like *Pdia3*, *Calr*, *Canx*, C/EBP (CCAAT/enhancer-binding protein) homologous protein (*Chop*) were estimated by qRT-PCR. To substantiate with the misfolded proteins in ER, the chaperones first refold themselves. The mRNA transcripts of *Ire1*, *Perk*, *Atf6*, *Pdia3*, *Canx*, *Calr*, and *Chop* of HFFD-fed rats showed an increase of 3.6-, 4.1-, 4.0-, 3.5-, 3.0-, 2.9-, and 3.8-fold, respectively, as compared to control rats. SPL supplementation resulted in a 3.2-, 3.3-, 3.3-, 2.9-, 2.3-, 2.4-, and 2.6-fold increase among the genes analyzed for ER stress whereas 4-PBA showed 2.0-, 1.9-, 1.7-, 1.8-, 1.7-, 1.7-, and 2.1-fold change as compared to the rats fed with standard pellet. Taken together, these observations provide evidence that lipid accumulation initiates ER stress in pancreatic islets (Fig. 2a–g).

SPL inhibits ER stress sensors and its downstream target proteins Having observed the effect of SPL on the ER chaperones mRNA transcripts, we then determined the canonical proteins of ER stress and the downstream targets through Western blot analysis. Elevated ER stress unbound GRP78 with the three sensor proteins and its upregulation phosphorylated and activated their downstream signaling proteins. Autophosphorylation of PERK led to the phosphorylation of eIF2α and activated ATF4 and CHOP expression in ER stressed rats. Phosphorylation of IRE1 increased the splicing of XBP1leading to the activation of GRP78 in HFFD-fed rats. The third ER sensor protein ATF6α gets dissociated from GRP78, cleaved at Golgi, and translocated to the nucleus after its activation by HFFD feeding. SPL or 4-PBA treatment brought back the protein expression levels nearer to the normal. Taken together, the results suggest that SPL modulates the expression of ER stress sensors and their downstream signaling target in HFFD-fed rats confirming the potential of SPL in alleviating the ER stress (Fig. 3a–d). Immunohistochemical studies also supported that SPL supplementation resulted in a significant decrease in the expression of phospho-IRE1 when SPL was supplemented to HFFD-fed rats (Fig. 4).

Phosphorylation status of JNK Next, we examined whether SPL rescues HFFD-induced over expression of JNK by assessing the phosphorylation status of JNK in HFFD-fed rats. Treatment with SPL or 4-PBA suppresses the expression of phospho-JNK$^{Thr183/Tyr185}$, an insulin signaling kinase (Fig. 5a, b). Increased expression of IRE1α leads to the activation of JNK thereby negatively regulates insulin signaling.

Ultrastructural imaging of the rat pancreas The ultrathin stained sections of β-cells of the control rats exhibit normal pattern of nuclei, endoplasmic reticulum, and mitochondria. While β-cell sections from HFFD-fed rat exhibit distended ER and rearranged pattern of cisternae. Upon treatment with SPL, the structure of organelles is rearranged as in normal rats (Fig. 6a–c). Twofold and 1.5-fold expansion in ER is observed among HFFD-fed rats and SPL-treated HFFD rats, respectively, through the Image J software.

Discussion

The current study expressed the effects of SPL on the excess nutrient-induced ER stress through in vitro and in vivo approaches. Both the results were consistent with each other showing an important role of SPL in controlling ER stress. Recent studies hint the involvement of obesity-induced ER stress as an important pathogenic factor for pancreatic β-cell failure (Back and Kaufman 2012; Laybutt et al. 2007). SPL has been proven to protect against methylglyoxal-induced hyperglycemia and insulin resistance in male Wistar rats (Lee et al. 2014). However, the mechanism of SPL action on ER stress remains unknown.

Amelioration of ER stress in vitro Palmitate is used extensively in in vitro studies to induce insulin resistance and its effects are attributed to its metabolites. β-cell dysfunction developed by ER stress in the pancreas was shown to be induced by saturated free fatty acids (Laybutt et al. 2007; Karaskov et al. 2006; Kharroubi et al. 2004). Phosphorylation and activation of PERK pathway is regulated differentially by extracellular glucose and palmitate treatment in β-cells. Earlier β-cells treated with palmitate induce the PERK pathway that involves the phosphorylation of eIF2α resulting in over expression of ATF4 and CHOP (Ozcan et al. 2004; Cnop et al. 2010).

IRE1α, a canonical ER stress sensor results in the alterations of its signaling genes due to prolonged ER stress (Okuda-Shimizu and Hendershot 2007). Chronic activation of IRE1α in β-cells by exposure to high-glucose cleaves unspliced *Xbp1* mRNA and insulin mRNA suggesting that IRE1α–*Xbp1* signaling is essential for β-cell function (Back and Kaufman 2012). Prolonged activation of IRE1α in ER of adipocytes might interrupt insulin signaling (Kawasaki et al. 2012). In addition to PERK and IRE1α, a study by Wang et al. (2009) has proved that acute ER stress induced phosphorylation of CREB-regulated transcription coactivator 2 (CRTC2) and enhanced gluconeogenesis by ATF6 overexpression.

Induction of ER stress by palmitate in RIN5f cells was found to be associated with elevated IRE1α, PERK, and ATF6α signaling transduction and its downstream signaling targets including the molecular chaperones. Importantly, all of these genes have been shown to be induced by ER stress caused by prolonged palmitate exposure in cultured mouse MIN6 cells (Laybutt et al. 2007). We examined the effect of SPL treatment on ER stress in RIN5f cells with palmitate-induced ER stress. The levels of phospho-forms of PERK and IRE1α and the

activation of ATF6α protein expression induced by palmitate were reversed by SPL to normal levels. These results indicate that SPL reduces palmitate-induced ER stress in vitro.

Attenuation of ER stress in Sprague Dawley rats Diets rich in high calories are the known inducers of UPR and pathological ER stress (Cnop et al. 2012). In pancreatic β-cells, ER stress has been induced by excess nutrients, amyloid deposits, and inflammatory cytokines (Eizirik et al. 2008) which are counteracted by the activation of UPR pathways particularly in high secretory cells like β-cells (Oyadomari and Mori 2004). In animal models, pancreatic β-cell death was evidenced by the perturbation of the UPR signaling (Harding et al. 2001; Scheuner et al. 2005; Zhang et al. 2002).

Proinsulin mRNA and protein synthesis is stimulated by prolonged high-glucose concentrations which resulted in the activation of PERK leading to protein entry into the ER (Hou et al. 2008). Alterations in the splicing of *Xbp1* which leads to β-cell failure in the β-cell-specific XBP1 mutant mice model were proved earlier by Lee et al. (2011). And also Seo et al. (2008) reported that under ER stress the ectopic over expression of ATF6α creates β-cells apoptosis. Multiple studies that use mice fed with high-fat diet report the involvement of eIF2α signaling (Birkenfeld et al. 2011) or IRE1α in induction of hepatic lipid accumulation and insulin resistance (Bailly-Maitre et al. 2010). Previous studies, in this context, have been well documented with the increased levels of eIF2α phosphorylation, splicing of XBP1 mRNA, and CHOP and GRP78 protein levels in the islets of mice with models of insulin resistance and beta cell failure (Laybutt et al. 2007). Furthermore, recent studies on ER stress accounted the significant increase in ER stress marker proteins, namely GRP78 and CHOP in islets of T2D individuals (Laybutt et al. 2007).

In our laboratory, earlier, we have reported that HFFD elevated the ER stress proteins IRE1α, PERK, ATF6α, XBP1s, and eIF2α in liver tissues (Bhuvaneswari et al. 2014). In the current observation, we confirmed that SPL inhibits ER stress signaling by downregulating IRE1α, PERK, and ATF6α by comparing the mechanism with 4-PBA, which has been already proved to downregulate IRE1α and PERK phosphorylation (Gregor and Hotamisligil 2007) and decrease ER stress markers GRP78, CHOP, ATF4, and XBP1s (Fonseca et al. 2012).

Role of JNK in pancreatic ER stress JNK activation and ER stress have been suggested as the major participants in the commencement of insulin resistance (Jaeschke and Davis 2007). In fact, in adipose tissue and liver of HFD-fed and ob/ob mice, increased phosphorylation of PERK and IRE1α and JNK activation are shown (Ozcan et al. 2004, 2009). Similarly we have obtained the results of JNK phosphorylation influenced by IRE1α in our present study. Recent reports clearly depict that SPL inhibits the phosphorylation of extracellular regulated kinase 1/2 (ERK1/2) and JNK but not the non-phosphorylated mitogen-activated protein kinases (MAPKs) (Yao et al. 2012). Previous studies show that SPL induces autophagy through activation of Akt by promoting transcription of forkhead homeobox type O (FoxO) in the nucleus (Nam and Kim 2015). Herein, we suggest that SPL inhibits JNK, a negative modulator of insulin signaling.

Conclusion

From the current observations, we conclude that how SPL controls ER proteostasis and the suppression of JNK is clearly depicted in Fig. 7. The levels of key markers of ER stress elevated by lipotoxic environment are lowered by SPL. Although, alleviating IRE1α, PERK, and ATF6α could be the possible mechanisms underlying the protective effects of SPL against palmitate/HFFD-induced ER stress. SPL also decreased JNK phosphorylation, caused by increase in splicing of *Xbp1* mRNA induced by the phosphorylation of IRE1α. The findings obtained in this study opens up several avenues for further research. Further, SPL bioavailability and pharmacokinetics still remains to be established. SPL should be examined for its anti-diabetic effect after it is analyzed for its dosage with respect to protection against ER stress. Further studies that characterize the functional changes treated with SPL are needed, if ER stress is to be targeted by SPL.

Acknowledgements The authors wish to thank DST-FIST and UGC-SAP for the infrastructure facilities developed in the Department of Biochemistry and Biotechnology, Annamalai University, for executing the present study. We also thank Dr. Pushpa Viswanathan, Professor and Head, Dept. of Electron Microscope, Adyar Cancer Research Institute, Chennai, for conducting the electron microscopic studies successfully.

Funding information This work was supported by Department of Science and Technology, Women Scientists Scheme-A, New Delhi, India under "Disha Programme for Women in Science" (SR/WOS-A/LS-1170/2014).

Compliance with ethical standards

Experimental procedures were approved by the Institutional Animal Ethics Committee (IAEC), Annamalai University, and conducted according to the guidelines by the Committee for the Purpose of Control and Supervision on Experiments on Animals (CPCSEA) (Proposal No. 1091).

Conflict of interest The authors declare that they have no conflicts of interest.

References

Adamopoulos C, Farmaki E, Spilioti E, Kiaris H, Piperi C, Papavassiliou AG (2014) Advanced glycation end-products induce endoplasmic reticulum stress in human aortic endothelial cells. Clin Chem Lab Med 52(1):151–160. https://doi.org/10.1515/cclm-2012-0826

Back SH, Kaufman RJ (2012) Endoplasmic reticulum stress and type 2 diabetes. Annu Rev Biochem 81:767–793. https://doi.org/10.1146/annurev-biochem-072909-095555

Bailly-Maitre B, Belgardt BF, Jordan SD, Coornaert B, von Freyend MJ, Kleinridders A, Mauer J, Cuddy M, Kress CL, Willmes D, Essig M, Hampel B, Protzer U, Reed JC, Bruning JC (2010) Hepatic Bax inhibitor-1 inhibits IRE1alpha and protects from obesity-associated insulin resistance and glucose intolerance. J Biol Chem 285(9):6198–6207. https://doi.org/10.1074/jbc.M109.056648

Bhuvaneswari S, Yogalakshmi B, Sreeja S, Anuradha CV (2014) Astaxanthin reduces hepatic endoplasmic reticulum stress and nuclear factor-kappaB-mediated inflammation in high fructose and high fat diet-fed mice. Cell Stress Chaperones 19(2):183–191. https://doi.org/10.1007/s12192-013-0443-x

Birkenfeld AL, Lee HY, Majumdar S, Jurczak MJ, Camporez JP, Jornayvaz FR, Frederick DW, Guigni B, Kahn M, Zhang D, Weismann D, Arafat AM, Pfeiffer AF, Lieske S, Oyadomari S, Ron D, Samuel VT, Shulman GI (2011) Influence of the hepatic eukaryotic initiation factor 2alpha (eIF2alpha) endoplasmic reticulum (ER) stress response pathway on insulin-mediated ER stress and hepatic and peripheral glucose metabolism. J Biol Chem 286(42):36163–36170. https://doi.org/10.1074/jbc.M111.228817

Boden G, Duan X, Homko C, Molina EJ, Song W, Perez O, Cheung P, Merali S (2008) Increase in endoplasmic reticulum stress-related proteins and genes in adipose tissue of obese, insulin-resistant individuals. Diabetes 57(9):2438–2444. https://doi.org/10.2337/db08-0604

Castro G, MF CA, Weissmann L, Quaresma PG, Katashima CK, Saad MJ, Prada PO (2013) Diet-induced obesity induces endoplasmic reticulum stress and insulin resistance in the amygdala of rats. FEBS Open Bio 3:443–449. https://doi.org/10.1016/j.fob.2013.09.002

Cnop M, Ladriere L, Igoillo-Esteve M, Moura RF, Cunha DA (2010) Causes and cures for endoplasmic reticulum stress in lipotoxic beta-cell dysfunction. Diabetes Obes Metab 12(Suppl 2):76–82. https://doi.org/10.1111/j.1463-1326.2010.01279.x

Cnop M, Foufelle F, Velloso LA (2012) Endoplasmic reticulum stress, obesity and diabetes. Trends Mol Med 18(1):59–68. https://doi.org/10.1016/j.molmed.2011.07.010

Eizirik DL, Cardozo AK, Cnop M (2008) The role for endoplasmic reticulum stress in diabetes mellitus. Endocr Rev 29(1):42–61. https://doi.org/10.1210/er.2007-0015

Fonseca SG, Urano F, Weir GC, Gromada J, Burcin M (2012) Wolfram syndrome 1 and adenylyl cyclase 8 interact at the plasma membrane to regulate insulin production and secretion. Nat Cell Biol 14(10):1105–1112. https://doi.org/10.1038/ncb2578

Gao D, Bambang IF, Putti TC, Lee YK, Richardson DR, Zhang D (2012) ERp29 induces breast cancer cell growth arrest and survival through modulation of activation of p38 and upregulation of ER stress protein p58IPK. Lab Investig J Tech Methods Pathol 92(2):200–213. https://doi.org/10.1038/labinvest.2011.163

Gregor MF, Hotamisligil GS (2007) Thematic review series: adipocyte biology. Adipocyte stress: the endoplasmic reticulum and metabolic disease. J Lipid Res 48(9):1905–1914. https://doi.org/10.1194/jlr.R700007-JLR200

Gregor MF, Yang L, Fabbrini E, Mohammed BS, Eagon JC, Hotamisligil GS, Klein S (2009) Endoplasmic reticulum stress is reduced in tissues of obese subjects after weight loss. Diabetes 58(3):693–700. https://doi.org/10.2337/db08-1220

Ham JR, Lee HI, Choi RY, Sim MO, Choi MS, Kwon EY, Yun KW, Kim MY, Lee MK (2016) Anti-obesity and anti-hepatosteatosis effects of dietary scopoletin in high-fat diet fed mice. J Funct Foods 25:433–446. https://doi.org/10.1016/j.jff.2016.06.026

Harding HP, Zeng H, Zhang Y, Jungries R, Chung P, Plesken H, Sabatini DD, Ron D (2001) Diabetes mellitus and exocrine pancreatic dysfunction in perk-/- mice reveals a role for translational control in secretory cell survival. Mol Cell 7(6):1153–1163

Hou ZQ, Li HL, Gao L, Pan L, Zhao JJ, Li GW (2008) Involvement of chronic stresses in rat islet and INS-1 cell glucotoxicity induced by intermittent high glucose. Mol Cell Endocrinol 291(1–2):71–78. https://doi.org/10.1016/j.mce.2008.03.004

Jaeschke A, Davis RJ (2007) Metabolic stress signaling mediated by mixed-lineage kinases. Mol Cell 27(3):498–508. https://doi.org/10.1016/j.molcel.2007.07.008

Jung IR, Choi SE, Jung JG, Lee SA, Han SJ, Kim HJ, Kim DJ, Lee KW, Kang Y (2015) Involvement of iron depletion in palmitate-induced lipotoxicity of beta cells. Mol Cell Endocrinol 407:74–84. https://doi.org/10.1016/j.mce.2015.03.007

Kadowaki H, Nishitoh H (2013) Signaling pathways from the endoplasmic reticulum and their roles in disease. Genes 4(3):306–333. https://doi.org/10.3390/genes4030306

Kalivarathan J, Chandrasekaran SP, Kalaivanan K, Ramachandran V, Carani Venkatraman A (2017) Apigenin attenuates hippocampal oxidative events, inflammation and pathological alterations in rats fed high fat, fructose diet. Biomed Pharmacother 89:323–331. https://doi.org/10.1016/j.biopha.2017.01.162

Karaskov E, Scott C, Zhang L, Teodoro T, Ravazzola M, Volchuk A (2006) Chronic palmitate but not oleate exposure induces endoplasmic reticulum stress, which may contribute to INS-1 pancreatic beta-cell apoptosis. Endocrinology 147(7):3398–3407. https://doi.org/10.1210/en.2005-1494

Kawasaki N, Asada R, Saito A, Kanemoto S, Imaizumi K (2012) Obesity-induced endoplasmic reticulum stress causes chronic inflammation in adipose tissue. Sci Rep 2:799. https://doi.org/10.1038/srep00799

Kharroubi I, Ladriere L, Cardozo AK, Dogusan Z, Cnop M, Eizirik DL (2004) Free fatty acids and cytokines induce pancreatic beta-cell apoptosis by different mechanisms: role of nuclear factor-kappaB and endoplasmic reticulum stress. Endocrinology 145(11):5087–5096. https://doi.org/10.1210/en.2004-0478

Kim I, Xu W, Reed JC (2008) Cell death and endoplasmic reticulum stress: disease relevance and therapeutic opportunities. Nat Rev Drug Discov 7(12):1013–1030. https://doi.org/10.1038/nrd2755

Laybutt DR, Preston AM, Akerfeldt MC, Kench JG, Busch AK, Biankin AV, Biden TJ (2007) Endoplasmic reticulum stress contributes to beta cell apoptosis in type 2 diabetes. Diabetologia 50(4):752–763. https://doi.org/10.1007/s00125-006-0590-z

Lee AS (2005) The ER chaperone and signaling regulator GRP78/BiP as a monitor of endoplasmic reticulum stress. Methods 35(4):373–381. https://doi.org/10.1016/j.ymeth.2004.10.010

Lee AH, Iwakoshi NN, Glimcher LH (2003) XBP-1 regulates a subset of endoplasmic reticulum resident chaperone genes in the unfolded protein response. Mol Cell Biol 23(21):7448–7459

Lee AH, Heidtman K, Hotamisligil GS, Glimcher LH (2011) Dual and opposing roles of the unfolded protein response regulated by IRE1alpha and XBP1 in proinsulin processing and insulin secretion. Proc Natl Acad Sci U S A 108(21):8885–8890. https://doi.org/10.1073/pnas.1105564108

Lee HI, Yun KW, Seo KI, Kim MJ, Lee MK (2014) Scopoletin prevents alcohol-induced hepatic lipid accumulation by modulating the AMPK-SREBP pathway in diet-induced obese mice. Metab Clin Exp 63(4):593–601. https://doi.org/10.1016/j.metabol.2014.01.003

Livak KJ, Schmittgen TD (2001) Analysis of relative gene expression data using real time quantitative PCR and the $2^{-\Delta\Delta CT}$ method. Methods 25:402–408. https://doi.org/10.1006/meth.2001.1262

Lowry OH, Rosebrough NJ, Farr AL, Randall RJ (1951) Protein measurement with the Folin phenol reagent. J Biol Chem 193(1):265–275

Meusser B, Hirsch C, Jarosch E, Sommer T (2005) ERAD: the long road to destruction. Nat Cell Biol 7(8):766–772. https://doi.org/10.1038/ncb0805-766

Mogana R, Teng-Jin K, Wiart C (2013) Anti-inflammatory, anticholinesterase, and antioxidant potential of scopoletin isolated from Canarium patentinervium Miq. (Burseraceae Kunth). Evid Based Complement Alternat Med 2013:734824. https://doi.org/10.1155/2013/734824

Moon PD, Lee BH, Jeong HJ, An HJ, Park SJ, Kim HR, Ko SG, Um JY, Hong SH, Kim HM (2007) Use of scopoletin to inhibit the production of inflammatory cytokines through inhibition of the IkappaB/NF-kappaB signal cascade in the human mast cell line HMC-1. Eur J Pharmacol 555(2–3):218–225. https://doi.org/10.1016/j.ejphar.2006.10.021

Mosmann T (1983) Rapid colorimetric assay for cellular growth and survival: application to proliferation and cytotoxicity assays. J Immunol Methods 65(1–2):55–63

Nam H, Kim MM (2015) Scopoletin has a potential activity for anti-aging via autophagy in human lung fibroblasts. Phytomedicine 22(3):362–368. https://doi.org/10.1016/j.phymed.2015.01.004

Okuda-Shimizu Y, Hendershot LM (2007) Characterization of an ERAD pathway for nonglycosylated BiP substrates, which require Herp. Mol Cell 28(4):544–554. https://doi.org/10.1016/j.molcel.2007.09.012

Oyadomari S, Mori M (2004) Roles of CHOP/GADD153 in endoplasmic reticulum stress. Cell Death Differ 11(4):381–389. https://doi.org/10.1038/sj.cdd.4401373

Ozcan U, Cao Q, Yilmaz E, Lee AH, Iwakoshi NN, Ozdelen E, Tuncman G, Gorgun C, Glimcher LH, Hotamisligil GS (2004) Endoplasmic reticulum stress links obesity, insulin action, and type 2 diabetes. Science 306(5695):457–461. https://doi.org/10.1126/science.1103160

Ozcan L, Ergin AS, Lu A, Chung J, Sarkar S, Nie D, Myers MG Jr, Ozcan U (2009) Endoplasmic reticulum stress plays a central role in development of leptin resistance. Cell Metab 9(1):35–51. https://doi.org/10.1016/j.cmet.2008.12.004

Panda S, Kar A (2006) Evaluation of the antithyroid, antioxidative and antihyperglycemic activity of scopoletin from Aegle marmelos leaves in hyperthyroid rats. Phytother Res 20(12):1103–1105. https://doi.org/10.1002/ptr.2014

Ron D, Walter P (2007) Signal integration in the endoplasmic reticulum unfolded protein response. Nat Rev Mol Cell Biol 8(7):519–529. https://doi.org/10.1038/nrm2199

Rutkowski DT, Kaufman RJ (2007) That which does not kill me makes me stronger: adapting to chronic ER stress. Trends Biochem Sci 32(10):469–476. https://doi.org/10.1016/j.tibs.2007.09.003

Scheuner D, Vander Mierde D, Song B, Flamez D, Creemers JW, Tsukamoto K, Ribick M, Schuit FC, Kaufman RJ (2005) Control of mRNA translation preserves endoplasmic reticulum function in beta cells and maintains glucose homeostasis. Nat Med 11(7):757–764. https://doi.org/10.1038/nm1259

Seo HY, Kim YD, Lee KM, Min AK, Kim MK, Kim HS, Won KC, Park JY, Lee KU, Choi HS, Park KG, Lee IK (2008) Endoplasmic reticulum stress-induced activation of activating transcription factor 6 decreases insulin gene expression via up-regulation of orphan nuclear receptor small heterodimer partner. Endocrinology 149(8):3832–3841. https://doi.org/10.1210/en.2008-0015

Siatka T, Kasparova M (2008) Effects of auxins on growth and scopoletin accumulation in cell suspension cultures of Angelica archangelica L. Ceska Slov Farm 57(1):17–20

Verma A, Dewangan P, Kesharwani D, Kela PS (2013) Hypoglycemic and hypolipidemic activity of scopoletin (coumarin derivative) in streptozotocin induced diabetic rats. Int J Pharm Sci Rev Res 22(1):79–83

Wang Y, Vera L, Fischer WH, Montminy M (2009) The CREB coactivator CRTC2 links hepatic ER stress and fasting gluconeogenesis. Nature 460(7254):534–537. https://doi.org/10.1038/nature08111

Yao X, Ding Z, Xia Y, Wei Z, Luo Y, Feleder C, Dai Y (2012) Inhibition of monosodium urate crystal-induced inflammation by scopoletin and underlying mechanisms. Int Immunopharmacol 14(4):454–462. https://doi.org/10.1016/j.intimp.2012.07.024

Ye J, Rawson RB, Komuro R, Chen X, Dave UP, Prywes R, Brown MS, Goldstein JL (2000) ER stress induces cleavage of membrane-bound ATF6 by the same proteases that process SREBPs. Mol Cell 6(6):1355–1364

Yogalakshmi B, Bhuvaneswari S, Sreeja S, Anuradha CV (2014) Grape seed proanthocyanidins and metformin act by different mechanisms to promote insulin signaling in rats fed high calorie diet. J Cell Commun Signal 8(1):13–22. https://doi.org/10.1007/s12079-013-0210-x

Yoshida H, Matsui T, Yamamoto A, Okada T, Mori K (2001) XBP1 mRNA is induced by ATF6 and spliced by IRE1 in response to ER stress to produce a highly active transcription factor. Cell 107(7):881–891

Zhang P, McGrath B, Li S, Frank A, Zambito F, Reinert J, Gannon M, Ma K, McNaughton K, Cavener DR (2002) The PERK eukaryotic initiation factor 2 alpha kinase is required for the development of the skeletal system, postnatal growth, and the function and viability of the pancreas. Mol Cell Biol 22(11):3864–3874